*Energy Storage and Conversion* 2025, 3(2), 3249.
https://doi.org/10.59400/esc3249

Article

# Calculation vs. estimation: Impact of internal resistance determination on SOC estimation accuracy in lithium-ion batteries

**Seyit Emre Özcan, Hayri Arabaci***

Department of Electrical and Electronics Engineering, Faculty of Technology, Selçuk University, Konya 42075, Turkey
*** Corresponding author:** Hayri Arabaci, hayriarabaci@selcuk.edu.tr

**CITATION**

Özcan SE, Arabaci H. Calculation vs. estimation: Impact of internal resistance determination on SOC estimation accuracy in lithium-ion batteries. Energy Storage and Conversion. 2025; 3(2): 3249. https://doi.org/10.59400/esc3249

**ARTICLE INFO**

Received: 16 May 2025
Accepted: 9 June 2025
Available online: 26 June 2025



**Abstract:** The electrical equivalent circuit model (ECM) is widely employed for state of charge (SOC) estimation in lithium-ion batteries. Among ECM-based approaches, the Thevenin equivalent circuit model (TECM) is particularly favored due to its computational efficiency and ease of parameter identification. TECM can be implemented in various configurations, with 1RC, 2RC, and 3RC structures being the most common. In these configurations, each RC unit consists of a resistor (R) and a capacitor (C) connected in parallel and incorporated into the circuit branch in series. As the number of RC branches increases, the computational burden of SOC estimation also rises. However, the improvement in estimation accuracy does not scale proportionally with the increased model complexity. A critical factor influencing the accuracy of SOC estimation is the precise determination of ECM parameters. A widely accepted principle suggests that when a parameter can be directly computed from the available data, it is preferable to use the calculated value rather than an estimated one. In line with this principle, this study directly calculates the internal resistance parameter ($R_0$), which is connected in series with the RC branches in TECM, using test data while estimating the remaining RC parameters. SOC estimation is conducted for 1RC, 2RC, and 3RC configurations, and results are compared with those obtained from ECMs where all parameters, including $R_0$, are estimated. To ensure a rigorous comparison, all estimations are performed using the nonlinear least squares method (LSM). The study employs test data from the US06 and UDDS driving cycles, and performance evaluation is conducted based on error distributions (box plots), root mean square error (RMSE), mean absolute error (MAE), and computational cost. The results showed that there is no significant difference between the error values of the predictions made using the model in which $R_0$ is directly calculated and those made using the model in which $R_0$ is estimated. Specifically, for the 1RC model structure, the lowest MAE values are 6.2 and 6.1 millivolts, respectively. However, these values indicate that the nonlinear LSM can be effectively used for estimating the parameters of the battery electrical circuit model.

**Keywords:** lithium-ion battery; Thevenin equivalent circuit model; hybrid pulse power characterization; state of charge; nonlinear LSM; parameter optimization

## 1. Introduction

Today, lithium-ion batteries are widely used in energy storage systems. They offer significant advantages, particularly in electric vehicles, renewable energy systems, and portable electronic devices, due to their high energy density, long cycle life, and fast charge-discharge capabilities. However, accurately modeling batteries and reliably predicting their performance are critical for both efficient energy management and optimizing battery lifespan.

The Battery Management System (BMS) is an electronic system designed to ensure the safe, efficient, and long-lasting operation of batteries. One of the most

critical factors determining the effectiveness of a BMS is its ability to estimate the SoC of the battery accurately. Accurate SoC estimation is a fundamental engineering challenge in battery management, directly impacting the performance of energy storage systems. Therefore, the development of SoC estimation methods is considered a critical research area for enhancing the reliability and sustainability of battery technologies. SoC, State of Health (SoH), and State of Available Power (SoAP) are the key battery states that need to be determined using monitoring algorithms [1].

SoC estimation in batteries has undergone a significant evolutionary process, ranging from the fundamental method of terminal voltage measurements to Coulomb counting, ECM-based approaches, and data-driven machine learning techniques. This progression enhances the reliability, accuracy, and efficiency of BMS, enabling energy storage systems to operate more effectively. Research on SoC estimation continues to advance alongside developments in battery technologies, significantly contributing to the optimization of energy storage system performance. SoC represents the available battery capacity and is one of the most critical parameters to monitor for optimizing battery performance and extending its lifespan [2]. Various model-based and data-driven methods, such as the Kalman Filter, Artificial Neural Networks, and Electrochemical Impedance Spectroscopy, can be employed for SoC estimation [3]. In ECM-based SoC estimation methods, accurately determining ECM parameters directly affects the accuracy of estimation algorithms and the performance of the energy extracted from the battery. Therefore, precise parameter identification is crucial. Utilizing more comprehensive battery ECMs enables more accurate and effective predictions of battery state and behavior [4].

The hybrid pulse power characterization (HPPC) test plays a crucial role in evaluating the performance of lithium-ion batteries, particularly in electric vehicles, energy storage systems, and other high-power applications. This test provides critical data on battery safety, durability, and efficiency, making it a fundamental analytical tool in the development of battery technologies. Additionally, HPPC test data are widely used for calculating ECM parameters and contribute significantly to enhancing the accuracy and effectiveness of BMS. These test data enable the application of various parameter estimation methods, ensuring the precise and reliable determination of battery parameters [5,6]. The parameter values obtained from HPPC tests may exhibit nonlinear characteristics. In such cases, curve-fitting methods are applied to ensure the regularization of parameter variations [7,8]. To analyze dynamic behaviors effectively, various model structures based on Thevenin's ECM are commonly used for battery ECMs [9,10]. The optimization processes of ECM parameters are typically performed offline [11]. The parameter values derived from HPPC test results are subjected to validation tests using different datasets. These validation tests are generally conducted with data collected from batteries subjected to standard driving cycles. Since the sampling frequency of the data affects computational complexity, ECMs should be designed with an appropriate data acquisition frequency to ensure accurate and efficient parameter estimation [12].

Accurately determining the parameters for the ECM alone is not sufficient. In addition, it is necessary to mathematically define the nonlinear relationship between the battery's open circuit voltage (OCV) and the SoC. While OCV can be directly

obtained from HPPC tests by measuring the voltage after a rest period, the corresponding SoC value is calculated using the Coulomb counting method [13].

There are various approaches for parameter optimization using HPPC data, including recursive LSM, Differential Evolution Algorithm, Improved Differential Evolution Algorithm (IDE), and hybrid algorithms incorporating the Extended Kalman Filter [14]. Among these, LSM has been the most widely used. Numerous studies have demonstrated that LSM and its variants are effective for estimating ECM parameters. One such variant is Partial Adaptive Forgetting Factor Recursive LSM, which has proven helpful for SoC estimation [15]. This method can be utilized to develop a battery model based on HPPC testing [16]. Another variant, the Genetic Factor-Based LSM, is effective for parameter estimation in a study conducted in [17]. According to the simulation results, the model achieved an average error value of 0.0258 V and a standard deviation of 0.0336, demonstrating high accuracy and stability. In a study presented in [18], another variant of LSM, the Improved Recursive LSM, was used for ECM parameter identification. During the battery discharge process, the model achieved a low RMSE of 0.0058 V and an MRE of 0.0906%, indicating highly accurate estimations. Additionally, for the online identification of ECM parameters in lithium-ion batteries used in electric vehicles, the Adaptive Forgetting Factor Recursive Least Squares (AFFRLS) algorithm has been applied in simulation processes [19].

In [20], a hybrid approach was proposed, combining Electrochemical Impedance Spectroscopy (EIS) and HPPC tests to analyze battery losses. Using the LSM, ECM parameter estimation was performed, yielding an RMSE of 5 mV and a maximum error of 27 mV. Different models were examined, leading to the development of both an ECM and an electrochemical model for predicting lithium-ion battery performance. Specifically, for eVTOL applications, battery performance was evaluated using the HPPC test, where the ECM showed a 3.8% error rate. In comparison, the electrochemical model (E-Chem) achieved a lower error rate of 1.1% [21]. In another study, the dynamic behavior of the ECM was tested using an extended HPPC (EHPPC) test. Optimization algorithms, including Particle Swarm Optimization (PSO), Grey Wolf Optimization (GWO), Harmony Search (HS), and Golden Eagle Optimization (GEO), were compared. Among these, PSO achieved the best results with the lowest RMSE (0.00188) [22]. These studies have demonstrated that LSM is a highly accurate method for identifying ECM parameters. In line with these findings, this study compares ECMs using 1RC, 2RC, and 3RC parallel circuit structures. To ensure the reliability of the results, parameter estimation was conducted using the least squares approach.

Electrical circuit-based approaches used to analyze battery behavior consist of electrical parameters, particularly R and C components. Although the structures of these models may vary, the parameters are generally derived from experimental test data, typically obtained through HPPC tests. It is evident that the accuracy of the test data directly influences the accuracy of the estimated parameters. To ensure the reliability of experimental data, high-accuracy current, voltage, and temperature sensors, along with robust data acquisition systems, are employed. These data are used both for parameter estimation and validation using different portions of the same experimental dataset. Therefore, the reliability of the experimental data is a

fundamental and widely accepted premise. Various methods are employed to estimate parameters using these data, and the accuracy of the estimation results depends on the reliability of the estimation method. However, such results are not exact computations; they are estimations and inherently contain a certain degree of error. Since experimental data are assumed to be accurate, calculations based directly on these test data may yield more precise results, as they rely on reliable experimental measurements. Nonetheless, not all parameter values can be directly computed from experimental data. For this reason, directly calculating parameters that can be determined through computation, rather than estimating them, provides more reliable results [23]. In equivalent circuit models (ECMs), the $R_0$ value can be directly computed from HPPC test data. However, this is not the case for the parameters of the parallel RC circuits, which require estimation. Therefore, in this study, it is proposed that the $R_0$ parameter be determined through direct calculation from HPPC test data, while the RC parameters are estimated.

Parameter estimations and computational processes were carried out using HPPC test data. Validation tests were conducted using data obtained from batteries operating under standard driving cycles, specifically the UDDS and US06 driving conditions. The performance of different ECM was evaluated by comparing terminal voltages. During the comparison process, RMSE and MAE were used as error metrics. Additionally, box plot graphs were employed to compare maximum overshoot and error concentration regions. Furthermore, the durations of estimation processes were recorded and compared. The results were presented and analyzed comparatively.

## 2. Materials and methods

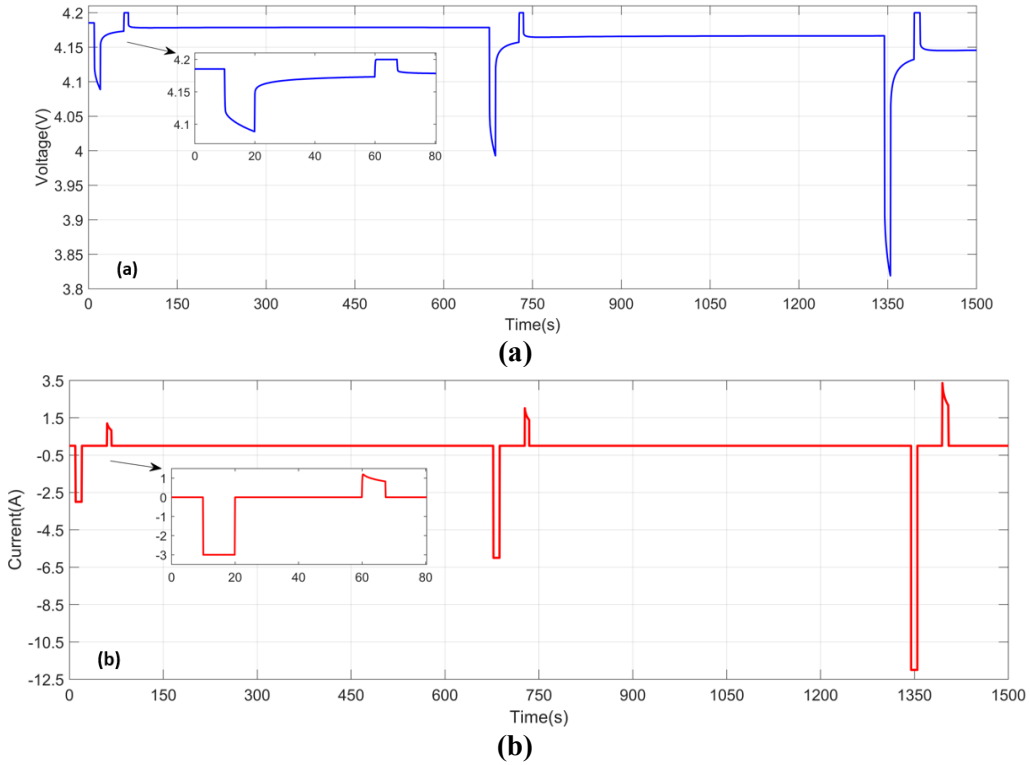


**Figure 1.** HPPC test curve: **(a)** voltage variation curve; **(b)** current variation curve.

In this study, ECM parameters were estimated using HPPC test data from an LG 18650HG2 3Ah lithium-ion battery. These parameters are crucial for modeling the electrical dynamic behavior of batteries and for developing BMS. To determine these parameters, the nonlinear LSM was utilized. The HPPC test is a methodology that employs different current pulses to determine key battery parameters such as internal resistance, capacitance, and energy efficiency. Through this test, the battery's dynamic response characteristics under load can be analyzed, enabling the development of an ECM. A portion of the HPPC test data, showing the variation of battery voltage in response to the drawn current, is presented in **Figure 1**.

Battery ECM-based methods provide a simple yet effective mathematical approach to modeling the electrical behavior of batteries by utilizing circuit elements such as resistors, capacitors, and voltage sources. In this study, a comprehensive analysis was conducted using 1RC, 2RC, and 3RC TECM to examine the dynamic characteristics of the battery. These models assist in identifying the battery's internal losses, polarization effects, and transient behavior. **Figure 2** illustrates the 1RC, 2RC, and 3RC used TECM models, respectively.

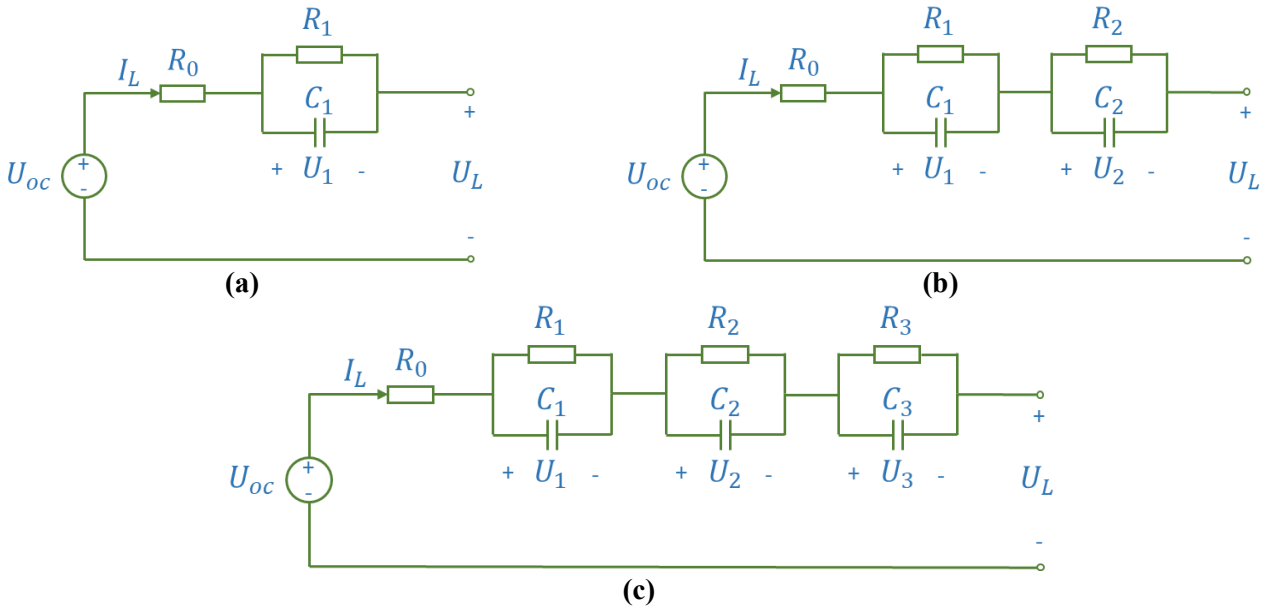


**Figure 2.** Thevenin equivalent circuit model **(a)** 1RC; **(b)** 2RC; **(c)** 3RC.

Due to their chemical nature, batteries cannot exhibit a voltage change that directly corresponds to the current passing through them. To better represent these dynamic behaviors, the Warburg impedance, consisting of resistive (R) and capacitive (C) elements, is utilized. Warburg impedance represents ion diffusion processes and models low-frequency behaviors in electrochemical systems. This impedance can be approximately modeled by connecting multiple resistor-capacitor (R-C) networks in series. Theoretically, an infinite number of resistor and capacitor networks would be required to form an exact equivalent of the Warburg impedance. However, this approach is impractical in real-world applications. Instead, in most cases, Warburg impedance can be successfully modeled using a limited number of R-C pairs within a specific frequency range. In the ECM, the series connection of R-C networks provides a more accurate and detailed representation of the voltage-current cycling process.

The estimation of parameters using HPPC test data was conducted following two distinct approaches. In the first approach, all parameters, including internal resistance ($R_0$), polarization resistance, and capacitance ($R_1$, $R_2$, $R_3$, and $C_1$, $C_2$, $C_3$), were estimated using nonlinear LSM. In the second approach, the $R_0$ parameter was directly calculated using a mathematical equation based on HPPC test data, while the remaining parameters ($R_1$, $R_2$, $R_3$, $C_1$, $C_2$, and $C_3$) were estimated using nonlinear LSM. The results of these two approaches were compared to assess the accuracy and reliability of the parameter estimations.

In a single cycle of the voltage variation curve of the HPPC test, as shown in **Figure 3**, points A-B represent the phase in which the battery transitions from its initial static, unloaded state to the stages of charging and discharging. During this process, the terminal voltage drops suddenly. Since the voltage across a capacitor cannot change instantaneously, the observed voltage drop occurs due to the internal resistance of the battery ($R_0$). Between points C and D, the pulse excitation ceases, the battery is no longer discharging, and it remains idle without any load. Additionally, due to polarization resistance, no abrupt voltage change is observed across the capacitor. The instantaneous voltage variation occurring in this phase is also attributed to $R_0$.

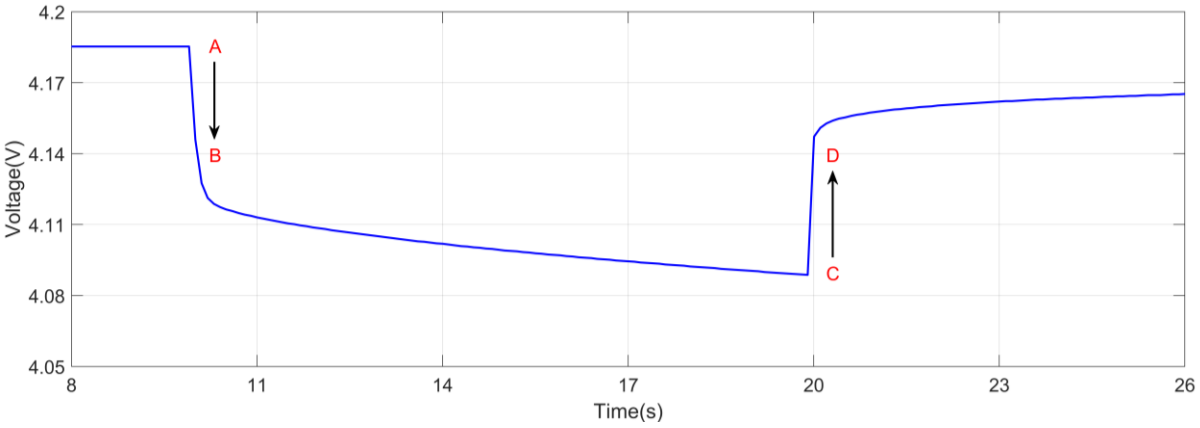


**Figure 3.** A single cycle of the HPPC test curve.

Both the voltage variations at points A-B and C-D reflect the characteristics of the $R_0$. The value of $R_0$ is obtained by dividing the voltage difference at these points by the discharge current. As shown in Equation (1), the average of these two segments is taken:

$$R_0 = \frac{(U_A - U_B) + (U_D - U_C)}{2I_L} \tag{1}$$

where $R_0$ represents the series internal resistance, while $U_A$, $U_B$, $U_C$, and $U_D$ denote the terminal voltage values at the moments when discharge and charge begin and end, respectively. Additionally, $I_L$ represents the current flowing through the battery terminal.

To establish the SoC-OCV relationship, the SoC is calculated during all current pulses in the HPPC test, as shown in Equation (2).

$$SoC_{k+1} = SoC_k - \frac{\eta_k \Delta t}{Q} I_{L,k} \tag{2}$$

where $k$ denotes the sample order, SoC denotes the state of charge, $\eta_k$ refers to the coulombic efficiency, $\Delta t$ is the sampling period, and $Q$ represents the battery capacity.

Establishing a relationship between the parameters through circuit analysis forms the foundation of the parameter identification approach. Subsequently, the LSM is applied to fit the parameters to the HPPC test results. The electrical behavior of the nRC circuit model can be described during the parameter identification process using Equations (3) and (4).

$$\dot{U}_n = -\frac{1}{R_n * C_n} U_n + \frac{1}{C_n} I_L \tag{3}$$

$$U_L = U_{oc} - I_L R_0 - \sum_{n=1}^{z} U_n \tag{4}$$

where $n$ represents the number of RC branches (1, 2, 3, …, ∞), $\dot{U}_n$ denotes the time derivative of the voltage across the RC branches, $R_n$ is the resistance of the RC branch, $C_n$ is the capacitance of the RC branch, $U_L$ is the battery terminal voltage, $U_{oc}$ represents the open circuit voltage of the battery, $I_L$ refers to the terminal current of the battery, $R_0$ is the series internal resistance, and $U_n$ represents the voltage across the RC branch.

When the differential equations presented in Equations (3) and (4) are solved and discretized, Equations (5) and (6) are obtained.

$$U_{n,k+1} = \left(e^{-\Delta t/R_n C_n}\right) U_{n,k} + R_n \left(1 - e^{-\Delta t/R_n C_n}\right) I_{L,k} \tag{5}$$

$$U_{L,k} = OCV(SoC_k) - \sum_{n=1}^{z} U_{n,k} - R_0 I_{L,k} \tag{6}$$

where $n$ represents the number of RC branches (1, 2, 3, …, ∞), $k$ donates the sample order, $U_n$ represents the voltage across the RC branch, $R_n$ and $C_n$ are the resistance and capacitance of the RC branch, $\Delta t$ refers to the sampling period, $U_L$ is the battery terminal voltage, $U_{oc}$ is the open circuit voltage, SoC indicates the state of charge during the current pulses, $I_L$ represents the battery terminal current, and $R_0$ denotes the series internal resistance.

As the number of parallel RC branches in the circuit increases, the order of the differential equations required for model analysis also increases. This results in higher mathematical complexity, makes the identification of circuit parameters more complicated, and raises the computational burden due to the increased number of operations during the solution process. This relationship is a significant factor in terms of model complexity. One of the aims of this study is to investigate the trade-off between model accuracy and computational complexity as the number of RC elements in the model increases.

RMSE is a widely used metric for evaluating the accuracy of model predictions. It fundamentally measures the differences between the predicted values of a model and the actual (measured) values. MAE computes the average of the absolute differences between actual and predicted values. These metrics are calculated using the mathematical expressions given in Equations (7) and (8).

$$\text{RMSE} = \sqrt{\frac{1}{N}\sum_{k=1}^{z}(y_i - \hat{y}_i)^2} \tag{7}$$

$$\text{MAE} = \frac{1}{N}\sum_{k=1}^{z}|y_i - \hat{y}_i| \tag{8}$$

where $k$ donates the sample order, N denotes the total number of samples, $y_i$ represents the measured terminal voltage data, and $\hat{y}_i$ represents the predicted terminal voltage data.

The calculation of internal resistance ($R_0$) was performed using the mathematical expression given in Equation (1) based on the HPPC test data. The computed $R_0$ value was then interpolated using the SoC calculation provided in Equation (2), allowing $R_0$ values to be obtained for all SoC levels. **Figure 4** presents a graphical representation of the variation of the calculated $R_0$ value with respect to SoC. Battery parameters exhibit a direct dependence on temperature. Specifically, resistive parameters ($R_0$, $R_1$, $R_2$, and $R_3$) tend to increase with rising temperature. In practical applications, it is essential to incorporate temperature-dependent parameters by leveraging data obtained from tests conducted at various temperature levels. However, since the primary objective of this study is to evaluate the proposed methodology, only experimental data acquired at 25 °C have been considered.

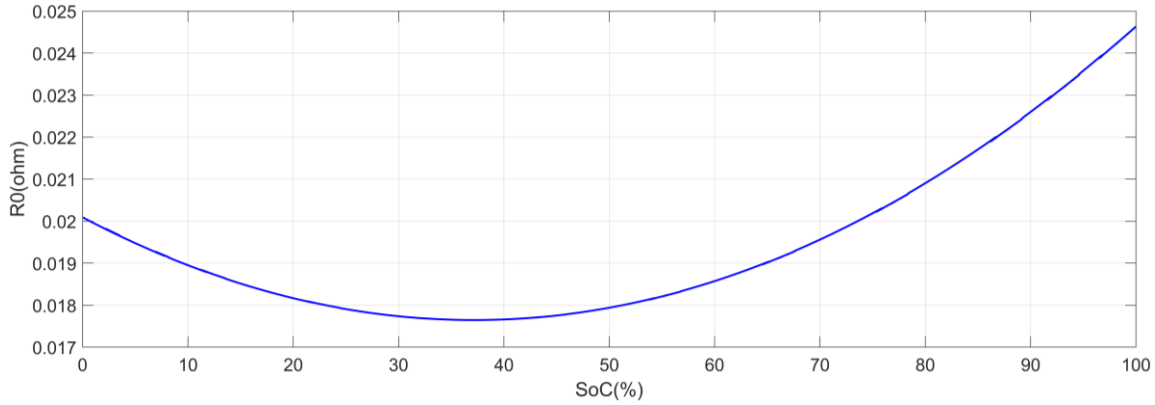


**Figure 4.** Variation of $R_0$ with SoC.

During the parameter estimation process, the initial $R_0$ value was determined by estimating it in a manner similar to other parameters ($R_n$, $C_n$). Additionally, for comparison purposes, the $R_0$ value calculated using the mathematical expression was used to estimate the other $R_n$ and $C_n$ parameters, completing the computations. The accuracy of the obtained parameters was validated through UDDS and US06 driving cycle tests, allowing for a detailed examination of the battery's dynamic response characteristics.

## 3. Experimental study

In this study, the effects of selecting ECM structures used in lithium battery simulations, as well as estimating and/or calculating parameters, on the accuracy of

SoC estimation were examined. Various analyses and comparisons were conducted. To validate the accuracy of the obtained ECM, current and voltage values, along with the corresponding SoC values, are required from a fully charged state to a fully discharged state. For the data to be applicable in real-world scenarios, particularly in electric vehicle applications, the discharge process must be performed using standard driving cycles.

In this study, datasets obtained using the UDDS, LA92, and US06 standard driving cycles, developed by the Battery Research Group at the University of Wisconsin-Madison, were utilized. These datasets are available on the Mendeley website [24]. The tests were conducted using an LG 18650HG2 cell with NMC chemistry and a 3.0 Ah capacity. In addition to the aforementioned driving cycles, tests were also performed using two hybrid driving cycles, and the corresponding data were collected. The datasets were recorded at a temperature of 25 ℃ with a sampling frequency of 10 Hz.

## 4. Results and discussion

The estimated parameter values, including the $R_0$ parameter, for the 1RC, 2RC, and 3RC ECMs are presented in **Table 1**. Additionally, the parameter values obtained using the $R_0$ value calculated through the mathematical equation are provided in **Table 2**.

**Table 1.** Estimated $R_0$ and 1RC, 2RC, and 3RC model parameter estimations.

| Model | 1RC | 2RC | 3RC |
|---|---|---|---|
| R0 | 0.0205 ohm | 0.0182 ohm | 0.0166 ohm |
| R1 | 0.0133 ohm | 0.0129 ohm | 0.0126 ohm |
| C1 | 1366.6 F | 1854.6 F | 2034.5 F |
| R2 | - | 0.0037 ohm | 0.0029 ohm |
| C2 | - | 425.7077 F | 992.9664 F |
| R3 | - | - | 0.0028 ohm |
| C3 | - | - | 91.3605 F |

**Table 2.** 1RC, 2RC, and 3RC model parameter estimations using the calculated $R_0$.

| Model | 1RC | 2RC | 3RC |
|---|---|---|---|
| R0 | 0.0199 ohm | 0.0199 ohm | 0.0199 ohm |
| R1 | 0.0132 ohm | 0.0123 ohm | 0.0124 ohm |
| C1 | 1222.4 F | 2171.4 F | 2101.9 F |
| R2 | - | 0.003 ohm | 0.0016 ohm |
| C2 | - | 1338.6 F | 2376.7 F |
| R3 | - | - | 0.0012 ohm |
| C3 | - | - | 2832.9 F |

When the results (**Table 1**) obtained from the initial approach are examined, it is observed that the value of $R_0$ decreases as the number of RC parallel branches increases. This implies that the voltage drops caused by the internal resistance are

represented with smaller values as the number of RC branches increases. However, when the total series ohmic resistance is considered—specifically $R_1$ for the 1RC model, $R_1 + R_2$ for the 2RC model, and $R_1 + R_2 + R_3$ for the 3RC model, including $R_0$—the values are 0.0338, 0.0348, and 0.0349, respectively. This indicates that although the voltage drop across $R_0$ decreases with the increase in RC branches, the total resistance remains nearly constant. Consequently, the steady-state voltage drop does not change significantly with the addition of more RC branches. On the other hand, under dynamic operating conditions, the decrease in voltage drop across $R_0$ and the corresponding increase in the voltage drops across $R_1$, $R_2$, and $R_3$ suggest that polarization-induced transient voltage drops are more accurately captured. Therefore, under usage conditions with variable profiles (such as in electric vehicles), it can be concluded that an equivalent circuit model with a higher number of RC branches yields more accurate results.

When examining the results obtained from the second approach (**Table 2**), it is observed that the value of $R_0$ remains constant as required by the approach, while the values of $R_1$ slightly decrease with an increasing number of RC branches. In this approach, since the value of $R_0$ is fixed across all equivalent circuit models, the voltage drop due to internal resistance remains constant. However, when the total series ohmic resistance is considered—specifically $R_1$ for the 1RC model, $R_1 + R_2$ for the 2RC model, and $R_1 + R_2 + R_3$ for the 3RC model, including $R_0$—the corresponding total resistance values are 0.0331, 0.0325, and 0.0351, respectively. This indicates a slight increase in overall resistance values. Accordingly, an increase in the number of RC branches may lead to greater voltage drops due to ohmic load in steady-state conditions. Additionally, the values of $R_2$ and $R_3$ in the 2RC and 3RC models remain very small, which limits the ability to capture voltage fluctuations in dynamic battery operation. This suggests that this approach may be relatively less suitable for applications involving variable profiles.

As a result of the parameter estimation process, the computation time required to estimate all parameters was first compared with that of the proposed approach. The comparison of optimization processes is presented in **Figure 5**, while the comparison of test durations for each value in the driving cycles is shown in **Figure 6**. The time required for the optimization process increases as the number of RC parallel branches grows. However, this increase is more significant than the proportional growth of the RC components. Nonetheless, considering that this optimization is performed only once per battery, its impact on online processing times is negligible. In practical applications, the SoC computation time per cycle is more critical in BMS. In this process, minimizing processor load and ensuring fast decision-making and response times in the BMS are crucial, making the shorter test durations more meaningful. As observed in **Figure 6**, the estimation times for the 1RC ECM model are consistently shorter than those for other models. The test durations of the proposed approach vary depending on the drive cycle; however, in the majority of tests, they are found to be shorter.

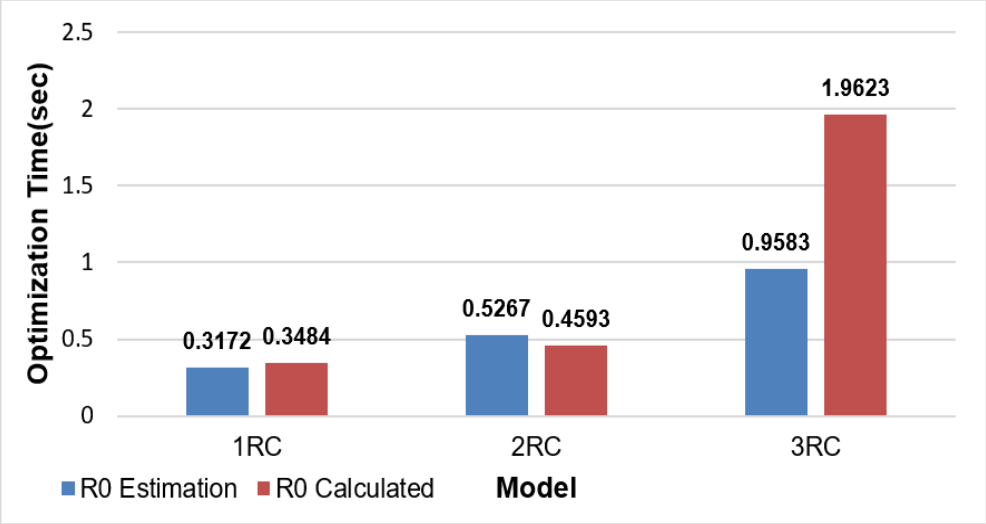


**Figure 5.** Optimization time graph.

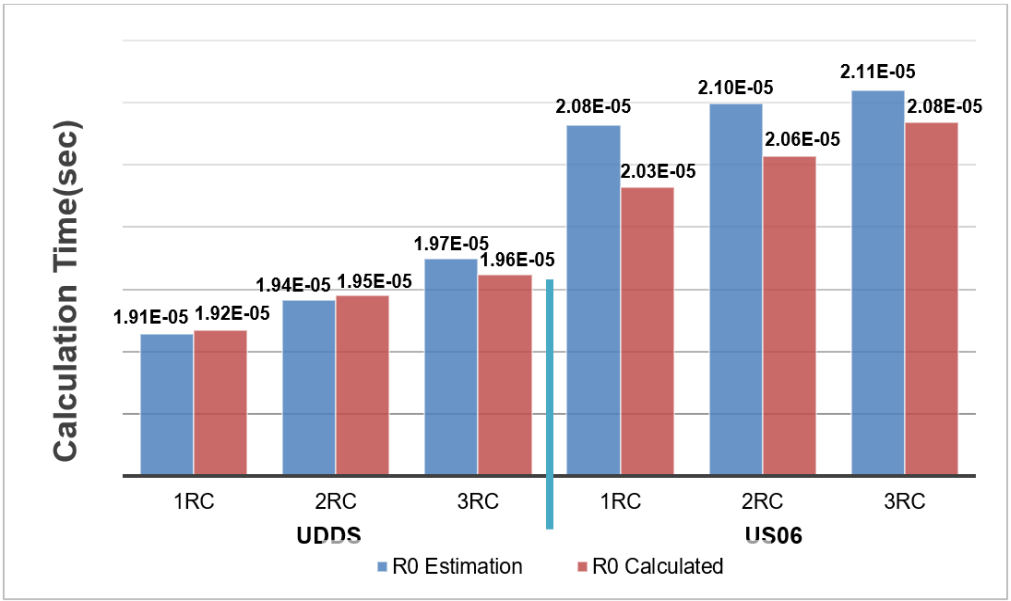


**Figure 6.** Processing time per operation in validation.

The validation study conducted using UDDS drive cycle test data includes a comparative analysis of the parameters of the 1RC, 2RC, and 3RC ECMs. The estimated values of all parameters, including the $R_0$ parameter, were obtained using the proposed approach. The verification results, along with the estimated parameters, are presented graphically in **Figure 7**.

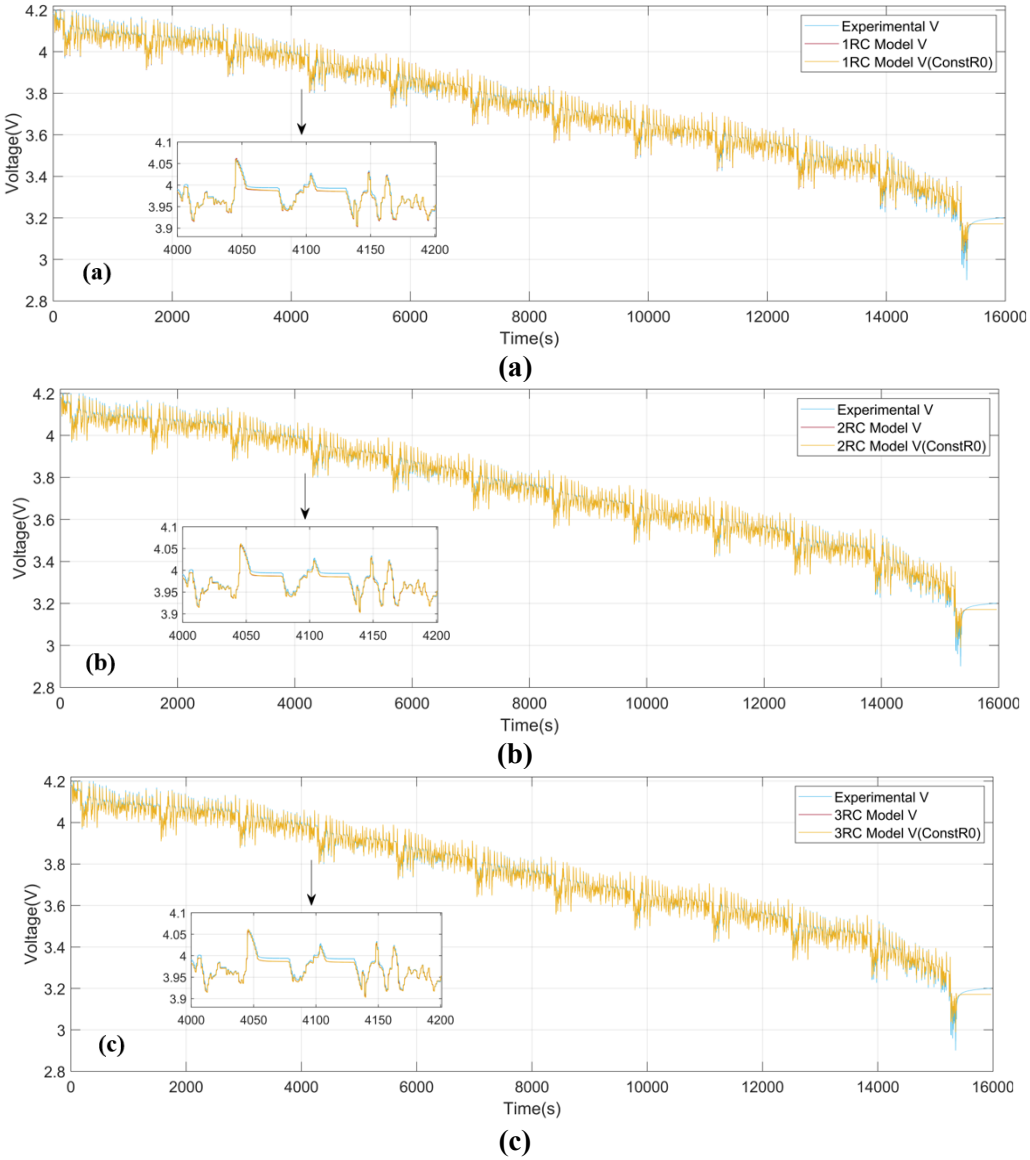


**Figure 7.** UDDS validation graphs **(a)** 1RC model; **(b)** 2RC model; **(c)** 3RC model.

According to the UDDS drive cycle validation results, the error rates between the estimated values, including the $R_0$ parameter, the values calculated using the proposed approach, and the actual data are presented in **Figure 8**. The obtained results indicate that, in both graphs, the error rate in the validation process decreases as the number of RC branches in the ECM increases. Additionally, it is observed that the error distribution and maximum overshoots are generally similar. This suggests that evaluating the results based on average errors is sufficient for decision-making.

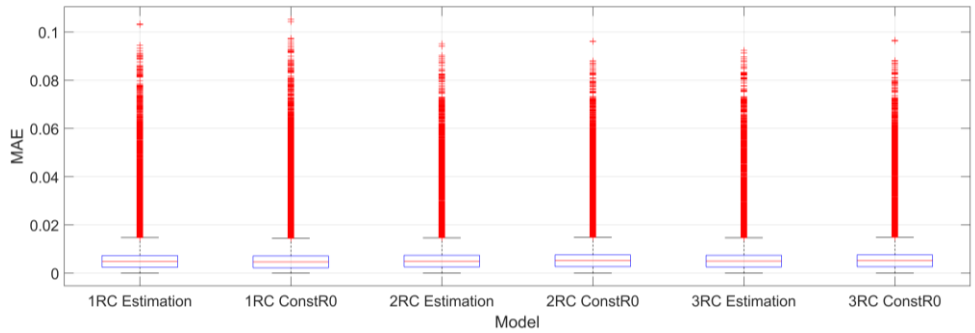


**Figure 8.** UDDS validation error graph.

The validation study conducted using US06 drive cycle test data includes a comparative analysis of the parameters of the 1RC, 2RC, and 3RC ECMs. The estimated terminal voltage values, obtained by predicting all parameters, including the R_0 parameter, are compared with the terminal voltage values obtained using the proposed approach. These comparisons are presented in **Figure 9**.

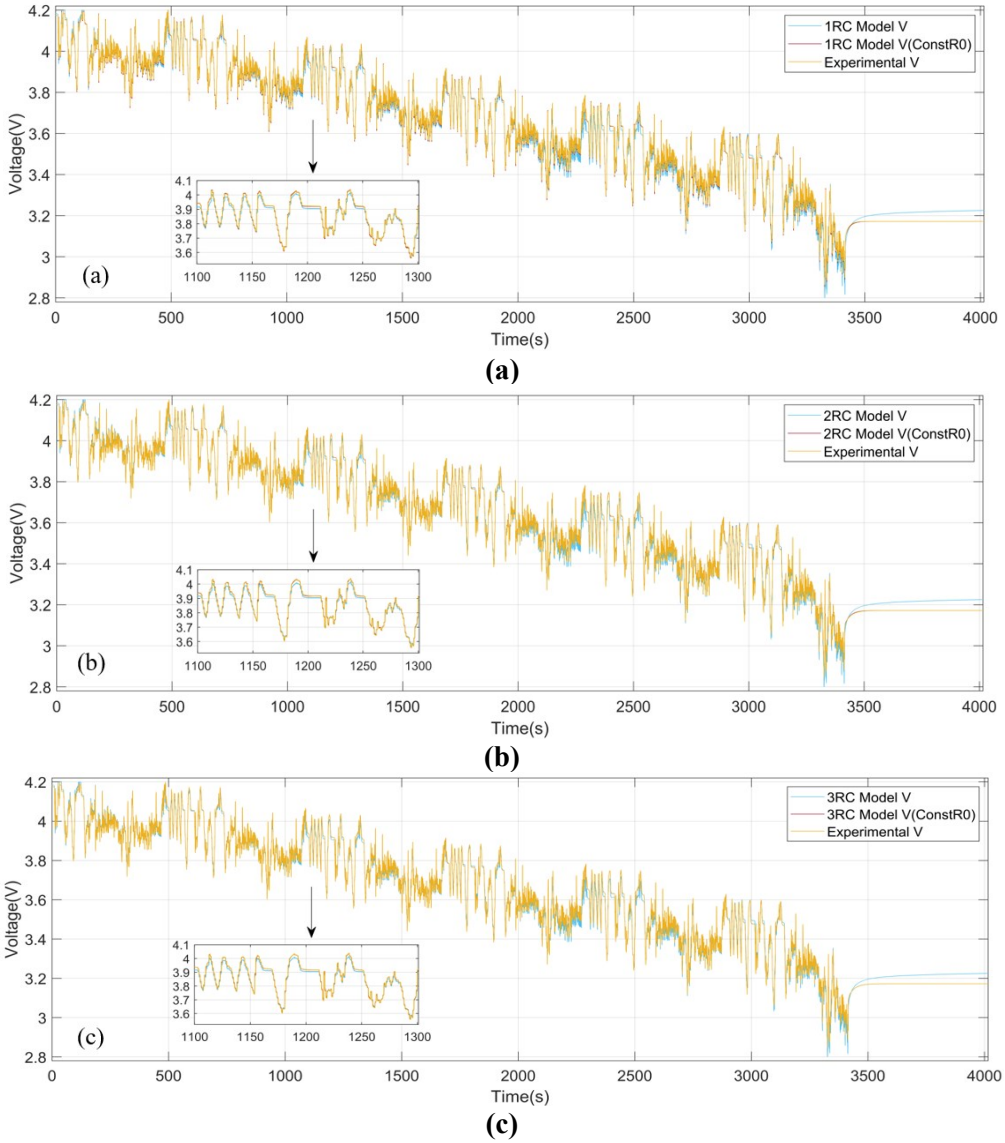


**Figure 9.** US06 validation graphs **(a)** 1RC model; **(b)** 2RC model; **(c)** 3RC model.

The error distribution obtained from the test results using the US06 drive cycle is presented in **Figure 10**. The results indicate that as the number of RC branches in the ECM increases, the error rate in the validation process decreases.

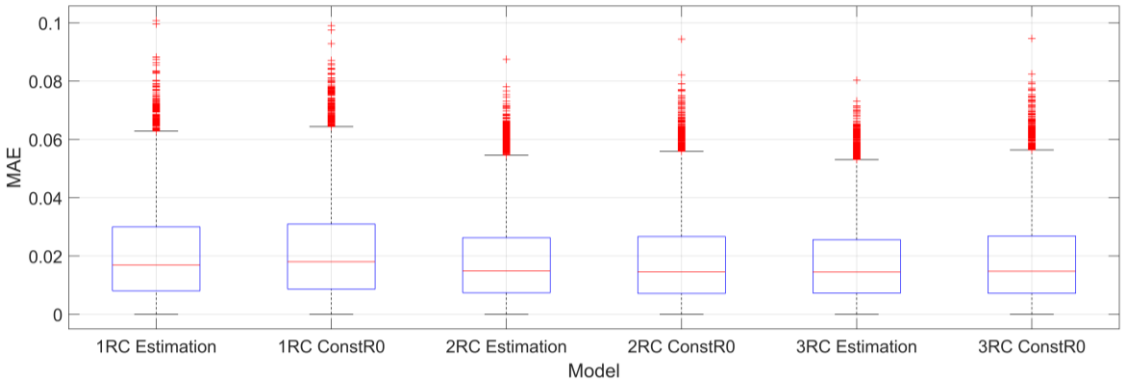


**Figure 10.** US06 validation error graph.

**Tables 3** and **4** present a comparison of error metrics (RMSE, MAE, and maximum error) calculated for different model configurations (1RC, 2RC, and 3RC) in the UDDS and US06 drive cycles. The results indicate that the model estimated using the 3RC configuration exhibits the lowest error values. However, although the maximum overshoot in the 3RC ConstR0 approach is more significant than that in the 3RC estimation, the difference is not substantial.

**Table 3.** RMSE, MAE, and maximum error values obtained by estimating all parameters.

| | **Error Voltage** | **1RC** | **2RC** | **3RC** |
|---|---|---|---|---|
| UDDS | RMSE | 0.0089 | 0.0086 | 0.0086 |
| | MAE | 0.0062 | 0.0061 | 0.0061 |
| | Max. Error | 0.1034 | 0.0951 | 0.0924 |
| US06 | RMSE | 0.0257 | 0.0237 | 0.0234 |
| | MAE | 0.0206 | 0.0187 | 0.0184 |
| | Max. Error | 0.1007 | 0.0875 | 0.0803 |

**Table 4.** RMSE, MAE, and maximum error values calculated by estimating the $R_0$ parameter.

| | **Error Voltage** | **1RC** | **2RC** | **3RC** |
|---|---|---|---|---|
| UDDS | RMSE | 0.0090 | 0.0087 | 0.0087 |
| | MAE | 0.0061 | 0.0063 | 0.0063 |
| | Max. Error | 0.1053 | 0.0963 | 0.0966 |
| US06 | RMSE | 0.0264 | 0.0238 | 0.0240 |
| | MAE | 0.0213 | 0.0188 | 0.0188 |
| | Max. Error | 0.0991 | 0.0944 | 0.0946 |

Considering the number of computations and processing time, the use of 1RC-based models appears to be more suitable. The slight differences in error values shown in **Figure 9** indicate that using the 1RC model does not significantly impact the

accuracy of SoC estimation. The key question here is, "Which approach should be used—1RC Estimation or 1RC ConstR0?" To answer this question, the MAE and RMSE values presented in **Tables 3** and **4** can be examined.

As observed from the tables, when all parameters are estimated (**Table 3**), the RMSE and MAE values are generally lower for the 2RC and 3RC models. Precisely, for the UDDS drive cycle, the RMSE value is calculated as 0.0089 for the 1RC model, whereas it decreases to 0.0086 for both the 2RC and 3RC models. A similar trend is observed for MAE, with the maximum error reaching its lowest level (0.0924) in the 3RC model. A comparable trend is also evident in the US06 cycle, where RMSE and MAE values exhibit a decreasing pattern from the 1RC model to the 3RC model. These findings demonstrate that more complex circuit models offer advantages in terms of error metrics.

When the $R_0$ parameter is calculated and used (**Table 4**), no significant change in error values is observed. For the UDDS drive cycle, the RMSE values for the 1RC, 2RC, and 3RC models are calculated as 0.0090, 0.0087, and 0.0087, respectively. Similarly, in the US06 drive cycle, the 3RC model exhibits the lowest RMSE value of 0.0240. However, when examining maximum error values, it is noteworthy that calculating the $R_0$ parameter can, in some cases, lead to an increase in error rates. For instance, in the US06 cycle, the maximum error value for the 3RC model is found to be 0.0803 in **Table 3**, whereas it increases to 0.0946 in **Table 4**.

In light of these findings, it is evident that the complexity of the circuit model in battery modeling has a direct impact on error metrics. Models incorporating a higher number of RC elements generally yield lower RMSE and MAE values. However, to examine how the 1RC, 2RC, and 3RC models are affected in terms of computational load, the time spent on SoC estimation, rather than the number of operations, was analyzed and recorded (**Figure 6**). In the comparisons and evaluations, time durations were taken as the basis. **Table 5** presents a comparison of estimation times versus MAE values for driving cycles. As shown in the table, error values decrease as the number of RC elements increases. On the other hand, the increase in computation time is relatively minimal. This indicates that the 3RC model can be preferred for higher accuracy. However, to fully understand the impact of computational load (or duration), SoC estimation should be performed on the processor used in the BMS for a more realistic assessment.

**Table 5.** Comparison of MAE and estimation times.

| | | **1RC** | **2RC** | **3RC** |
|---|---|---|---|---|
| UDDS | MAE [V] | 0.0062 | 0.0061 | 0.0061 |
| | Est. Time [s] | $1.91 \times 10^{-5}$ | $1.94 \times 10^{-5}$ | $1.97 \times 10^{-5}$ |
| US06 | MAE [V] | 0.0206 | 0.0187 | 0.0184 |
| | Est. Time [s] | $2.08 \times 10^{-5}$ | $2.10 \times 10^{-5}$ | $2.11 \times 10^{-5}$ |

Similarly, the approach of explicitly calculating the $R_0$ parameter had no significant effect on model accuracy, but it was observed to increase the maximum error values in specific scenarios. This highlights the importance of carefully considering parameter estimation methods and model selection in the battery modeling

process. The tests presented here were conducted using high-capacity computers, with processing times of approximately 20 microseconds. Considering that processors would perform these operations within a BMS, which are typically low-capacity (likely 32-bit microcontrollers), the processing times would be significantly longer. Therefore, using the 1RC model would be a more appropriate choice. Moreover, the fact that there is no significant difference in accuracy between the 1RC model and the 3RC model indicates that the 1RC model would be more practical in real-world applications.

## 5. Conclusion

In this study, the parameters of the 1RC, 2RC, and 3RC ECMs were determined using HPPC test data via nonlinear LSM. To evaluate the accuracy of the model parameters, standard drive cycles, specifically US06 and UDDS tests, were conducted, and the results were analyzed comparatively. The results show that estimation accuracy improves with increasing model complexity (from 1RC to 3RC) for all parameters. Similarly, when using the calculated $R_0$ parameter value, an improvement in estimation accuracy is observed as model complexity increases. However, this increase in model complexity also leads to longer computation times.

While more complex models better represent the dynamic behavior of the battery, the increased computational cost may impose performance limitations in real-time applications. RMSE, MAE, and maximum error results indicate that the 1RC model offers an optimum balance in terms of accuracy and computational load in systems using processors with low processing power.

In future work, the proposed direct computation method for $R_0$ can be integrated into the Extended Kalman Filter or other real-time adaptive filtering frameworks to enhance the robustness and adaptability of state estimation in dynamic operating conditions.

**Author contributions:** Conceptualization, HA and SEO; methodology, HA; software, SEO; validation, SEO and HA; formal analysis, HA; investigation, SEO; resources, SEO; data curation, HA; writing—original draft preparation, HA; writing—review and editing, HA; visualization, SEO; supervision, HA; project administration, HA; funding acquisition, HA. All authors have read and agreed to the published version of the manuscript.

**Institutional review board statement:** Not applicable.

**Informed consent statement:** Not applicable.

**Conflict of interest:** The authors declare no conflict of interest.

## References

1. Farmann A, Sauer DU. Comparative study of reduced order equivalent circuit models for on-board state-of-available-power prediction of lithium-ion batteries in electric vehicles. Applied Energy. 2018; 225: 1102-1122. doi: 10.1016/j.apenergy.2018.05.066
2. Rivera-Barrera J, Muñoz-Galeano N, Sarmiento-Maldonado H. SoC Estimation for Lithium-ion Batteries: Review and Future Challenges. Electronics. 2017; 6(4): 102. doi: 10.3390/electronics6040102

3. Kumar RR, Bharatiraja C, Udhayakumar K, et al. Advances in Batteries, Battery Modeling, Battery Management System, Battery Thermal Management, SOC, SOH, and Charge/Discharge Characteristics in EV Applications. IEEE Access. 2023; 11: 105761-105809. doi: 10.1109/access.2023.3318121
4. Shen M, Gao Q. A review on battery management system from the modeling efforts to its multiapplication and integration. International Journal of Energy Research. 2019; 43(10): 5042-5075. doi: 10.1002/er.4433
5. Xiong R, Cao J, Yu Q, et al. Critical Review on the Battery State of Charge Estimation Methods for Electric Vehicles. IEEE Access. 2018; 6: 1832-1843. doi: 10.1109/access.2017.2780258
6. Adaikkappan M, Sathiyamoorthy N. Modeling, state of charge estimation, and charging of lithium-ion battery in electric vehicle: A review. International Journal of Energy Research. 2021; 46(3): 2141-2165. doi: 10.1002/er.7339
7. Jung S, Tullu A. Characteristics Evaluation of 14 Battery Equivalent Circuit Models. IEEE Access. 2023; 11: 117200-117209. doi: 10.1109/access.2023.3325395
8. Miniguano H, Barrado A, Lazaro A, et al. General Parameter Identification Procedure and Comparative Study of Li-Ion Battery Models. IEEE Transactions on Vehicular Technology. 2020; 69(1): 235-245. doi: 10.1109/tvt.2019.2952970
9. Karimi D, Behi H, Van Mierlo J, et al. Equivalent Circuit Model for High-Power Lithium-Ion Batteries under High Current Rates, Wide Temperature Range, and Various State of Charges. Batteries. 2023; 9(2): 101. doi: 10.3390/batteries9020101
10. Tran MK, DaCosta A, Mevawalla A, et al. Comparative Study of Equivalent Circuit Models Performance in Four Common Lithium-Ion Batteries: LFP, NMC, LMO, NCA. Batteries. 2021; 7(3): 51. doi: 10.3390/batteries7030051
11. Li Z, Shi X, Shi M, et al. Investigation on the Impact of the HPPC Profile on the Battery ECM Parameters' Offline Identification. In: Proceedings of the 2020 Asia Energy and Electrical Engineering Symposium (AEEES); 2020.
12. Zhang H, Deng C, Zong Y, et al. Effect of Sample Interval on the Parameter Identification Results of RC Equivalent Circuit Models of Li-ion Battery: An Investigation Based on HPPC Test Data. Batteries. 2022; 9(1): 1. doi: 10.3390/batteries9010001
13. Cipin R, Toman M, Prochazka P, et al. Identification of Li-ion Battery Model Parameters. In: Proceedings of the 2019 International Conference on Electrical Drives & Power Electronics (EDPE); 2019.
14. Reddy AKVK, Shekhar S, Narayana KVL, et al. An Improved Differential Evolution for Offline Parameter Estimation in Lithium-Ion Batteries with Real-World Usage Data. In: Proceedings of the 2023 Innovations in Power and Advanced Computing Technologies (i-PACT); 2023.
15. Liu S, Wang J, Liu Q, et al. Deep-Discharging Li-Ion Battery State of Charge Estimation Using a Partial Adaptive Forgetting Factors Least Square Method. IEEE Access. 2019; 7: 47339-47352. doi: 10.1109/access.2019.2909274
16. Huang Y, Li Y, Jiang L, et al. Research on Fitting Strategy in HPPC Test for Li-ion battery. In: Proceedings of the 2019 IEEE Sustainable Power and Energy Conference (iSPEC); 2019.
17. Wu Y, Chen H, Cao L, et al. Research on Online Identification of Lithium-ion Battery Equivalent Circuit Model Parameters. In: Proceedings of the 2022 9th International Forum on Electrical Engineering and Automation (IFEEA); 2022.
18. Ren B, Xie C, Sun X, et al. Parameter identification of a lithium-ion battery based on the improved recursive least square algorithm. IET Power Electronics. 2020; 13(12): 2531-2537. doi: 10.1049/iet-pel.2019.1589
19. Sun X, Ji J, Ren B, et al. Adaptive Forgetting Factor Recursive Least Square Algorithm for Online Identification of Equivalent Circuit Model Parameters of a Lithium-Ion Battery. Energies. 2019; 12(12): 2242. doi: 10.3390/en12122242
20. Koseoglou M, Tsioumas E, Panagiotidis I, et al. A lithium-ion battery equivalent circuit model based on a hybrid parametrization approach. Journal of Energy Storage. 2023; 73: 109051. doi: 10.1016/j.est.2023.109051
21. Qasem M, Stoyanov S, Ratrout S, et al. Synthetic Data-Integrated Li-Ion Battery Modeling for eVTOL Energy Systems. IEEE Access. 2024; 12: 76329-76343. doi: 10.1109/access.2024.3407016
22. Cheng YS. Identification of parameters for equivalent circuit model of Li-ion battery cell with population based optimization algorithms. Ain Shams Engineering Journal. 2024; 15(3): 102481. doi: 10.1016/j.asej.2023.102481
23. Plett GL. Battery management systems, Volume I: Battery modeling. Artech House; 2015.
24. Kollmeyer P, Vidal C, Naguib M, Skells M. LG 18650HG2 Li-ion battery data and example deep neural network xEV SOC estimator script. Mendeley Data. 2020; 3: 2020.